



## University of Dundee

Human metabolism of the semi-synthetic cannabinoids hexahydrocannabinol, hexahydrocannabiphorol and their acetates using hepatocytes and urine samples

Lindbom, Karin; Norman, Caitlyn; Baginski, Steven; Krebs, Lucas; Stalberga, Darta; Rautio, Tobias

*Published in:*  
Drug Testing and Analysis

*DOI:*  
[10.1002/dta.3740](https://doi.org/10.1002/dta.3740)

*Publication date:*  
2024

*Licence:*  
CC BY-NC

*Document Version*  
Publisher's PDF, also known as Version of record

[Link to publication in Discovery Research Portal](#)

*Citation for published version (APA):*

Lindbom, K., Norman, C., Baginski, S., Krebs, L., Stalberga, D., Rautio, T., Wu, X., Kronstrand, R., & Gréen, H. (2024). Human metabolism of the semi-synthetic cannabinoids hexahydrocannabinol, hexahydrocannabiphorol and their acetates using hepatocytes and urine samples. *Drug Testing and Analysis*. Advance online publication. <https://doi.org/10.1002/dta.3740>

**General rights**









Copyright and moral rights for the publications made accessible in Discovery Research Portal are retained by the authors and/or other copyright owners and it is a condition of accessing publications that users recognise and abide by the legal requirements associated with these rights.

**Take down policy**

If you believe that this document breaches copyright please contact us providing details, and we will remove access to the work immediately and investigate your claim.

## RESEARCH ARTICLE

# Human metabolism of the semi-synthetic cannabinoids hexahydrocannabinol, hexahydrocannabiphorol and their acetates using hepatocytes and urine samples

Karin Lindbom<sup>1</sup> | Caitlyn Norman<sup>1</sup>  | Steven Baginski<sup>2</sup>  | Lucas Krebs<sup>3</sup>  |  
 Darta Stalberga<sup>1</sup>  | Tobias Rautio<sup>4</sup>  | Xiongyu Wu<sup>4</sup>  |  
 Robert Kronstrand<sup>1,5</sup>  | Henrik Gréen<sup>1,5</sup> 

<sup>1</sup>Division of Clinical Chemistry and Pharmacology, Department of Biomedical and Clinical Sciences, Linköping University, Linköping, Sweden

<sup>2</sup>Leverhulme Research Centre for Forensic Science, School of Science and Engineering, University of Dundee, Dundee, UK

<sup>3</sup>Institute for Chemistry and Bioanalytics, School of Life Sciences, University of Applied Sciences Northwestern Switzerland, Muttenz, Switzerland

<sup>4</sup>Department of Physics, Chemistry and Biology, Linköping University, Linköping, Sweden

<sup>5</sup>Department of Forensic Genetics and Forensic Toxicology, National Board of Forensic Medicine, Linköping, Sweden

## Correspondence

Henrik Gréen, Division of Clinical Chemistry and Pharmacology, Department of Biomedical and Clinical Sciences, Linköping University, Linköping, Sweden.

Email: [henrik.green@liu.se](mailto:henrik.green@liu.se)

## Funding information

European Commission, Grant/Award Number: E! 113377; European Union's Horizon 2020; Sweden's Innovation Agency, Grant/Award Number: 2019-03566; Strategic Research Area in Forensic Sciences (Strategiområdet forensiska vetenskaper) at Linköping University; Leverhulme Trust, Grant/Award Number: RC-2015-011

## Abstract

Hexahydrocannabinol (HHC), hexahydrocannabiphorol (HHCP) and their acetates, HHC-O and HHCP-O, respectively, are emerging in Europe as alternatives to tetrahydrocannabinol (THC). This study aimed to elucidate the metabolic pathways of the semi-synthetic cannabinoids HHC, HHCP, HHC-O and HHCP-O from incubation with human hepatocytes. The metabolites of HHC were also identified in authentic urine samples. HHC, HHCP, HHC-O and HHCP-O were incubated with primary human hepatocytes for 1, 3 and 5 h. Authentic urine samples from cases screened positive for cannabis in blood using ELISA but confirmed negative were analysed both non-hydrolysed and hydrolysed for HHC metabolites. Potential metabolites were identified using ultra-high performance liquid chromatography (UHPLC) coupled to a quadrupole time-of-flight mass spectrometer (QToF-MS). HHC and HHCP were primarily metabolised through monohydroxylation (monoOH), followed by oxidation to a carboxylic acid metabolite. HHC-O and HHCP-O were rapidly metabolised to HHC and HHCP, respectively. In authentic urine samples, 18 different metabolites were identified, and 99.3% of hydroxylated metabolites were glucuronidated. 11-OH-HHC, 5'OH-HHC and another metabolite with a monoOH on the side chain were the only metabolites present in all 16 urine samples. The metabolism of HHC and HHCP were similar, although the longer alkyl side chain of HHCP (heptyl) led to greater hydroxylation on the side chain than HHC (pentyl). The use of HHC and HHCP can be differentiated from the use of THC and other phytocannabinoids, but the use of the acetate analogues may not be differentiable from their non-acetate analogues.

## KEYWORDS

hexahydrocannabinol, hexahydrocannabiphorol, HHC acetate, HHCP acetate, metabolism

Karin Lindbom and Caitlyn Norman contributed equally to this work.

This is an open access article under the terms of the [Creative Commons Attribution-NonCommercial](https://creativecommons.org/licenses/by-nc/4.0/) License, which permits use, distribution and reproduction in any medium, provided the original work is properly cited and is not used for commercial purposes.

© 2024 The Author(s). *Drug Testing and Analysis* published by John Wiley & Sons Ltd.

## 1 | INTRODUCTION

Hexahydrocannabinol (HHC), hexahydrocannabiphorol (HHCP) and their corresponding acetates, HHC-O and HHCP-O, respectively (see Figure 1 for chemical structures), are emerging as analogues to tetrahydrocannabinol (THC) and are marketed as new cannabis alternatives. These compounds have been sold in a variety of forms, for example, gummies, bubble gums, vapes or crude material.<sup>1</sup> HHC was first identified in Europe in May 2022<sup>2</sup> and has now been identified in a qualified majority of the EU Member States.<sup>1</sup> HHC-O has also emerged on the illicit market in Europe as an alternative to HHC with the first seizures reported in August 2022.<sup>3</sup> HHCP was discovered in November 2022,<sup>4</sup> and although no detections have been confirmed to date, HHCP-O has been reported to be available for sale on the illicit market.<sup>5</sup>

Chemically, HHC and its analogues are categorised as tricyclic terpenoid derivatives with a benzopyran ring (or hexahydrobenzochromenes). Although HHC and HHCP are found in small amounts in *Cannabis sativa*,<sup>6,7</sup> the HHC and HHCP detected on the market are synthesised from cannabidiol (CBD) and  $\Delta^9$ -tetrahydrocannabiphorol (THCP), respectively; therefore, they are classed as semi-synthetic cannabinoids.<sup>8,9</sup> The synthetic route of HHC-O and HHCP-O has not yet been reported but is likely synthesised using a similar method used for the synthesis of THC acetates.<sup>1</sup>

HHC has three stereocentres and eight possible stereoisomers<sup>8</sup>; however, it is typically only found as a mixture of two epimers, (9*R*) and (9*S*).<sup>8</sup> In HHC- and HHC-O-containing products, the (9*R*) epimer was found to be about twice as abundant as the (9*S*).<sup>8–11</sup> The (9*R*) epimer has also been found to be about twice as abundant as the (9*S*) in plasma and serum samples.<sup>12</sup> Although there is no pharmacodynamic activity data available for HHCP, HHC-O or HHCP-O, *in vivo* and *in vitro* studies of (9*R*)- and (9*S*)-HHC found both epimers were partial agonists of the human cannabinoid 1 and 2 (CB<sub>1</sub> and CB<sub>2</sub>) receptors. However, (9*R*)-HHC had much stronger binding affinity, potency and

cannabimimetic effects,<sup>8,13–15</sup> demonstrating that the intensity of biological effects can vary based on the epimeric mixtures, which is likely also true for HHC-O.

There is also limited information available on the pharmacokinetics and metabolism of HHC in humans and animals. Harvey and Brown (1991) examined the *in vitro* metabolism of (9*R*)-HHC using GC-MS in hepatic/liver microsomal preparations from five mammalian species. This study found only hydroxylated metabolites, where hydroxylation at the 11 position (11-OH-HHC) and 8 position (8-OH-HHC) were dominant. However, hydroxylation at all five positions on the *n*-pentyl side chain and the 4 carbon position on the aromatic ring was also found.<sup>16</sup> In a recent study reporting metabolite identification in a human urine sample after ingestion of 20 mg HHC, many of the identified metabolites were glucuronidated and the tentatively identified 4'-OH-HHC was found to be the major metabolite, followed by 11-OH-HHC and 8-OH-HHC.<sup>15</sup> Another study found (9*R*)-11-COOH-HHC to be the major metabolite in two urine samples after inhalation of 25 mg HHC, followed by (9*S*)-11-COOH-HHC, (9*R*)-11-OH-HHC and 9 $\alpha$ -OH-HHC.<sup>17</sup> Another study found 11-OH-HHC to be the major hydroxylated metabolite in a human blood sample and following pooled human liver S9 fraction incubations. No glucuronidated metabolites or 8-OH-HHC were found, but a carboxy metabolite was found in the human blood sample.<sup>18</sup> Although HHC-O and HHCP-O are believed to go through rapid metabolism and conversion to HHC and HHCP, respectively, *in vivo*, as seen for other esters, this metabolism has not yet been shown.

This study aimed to identify the main metabolites of HHC, HHCP and their corresponding acetates following incubation with human hepatocytes to get a more complete understanding of the human *in vitro* metabolism of these emerging semi-synthetic cannabinoids. In addition, the metabolites of HHC in authentic urine samples were identified, and the epimer composition of the (S)- and (R)-hydroxylated and carboxylic acid metabolites in these samples were chromatographically identified.

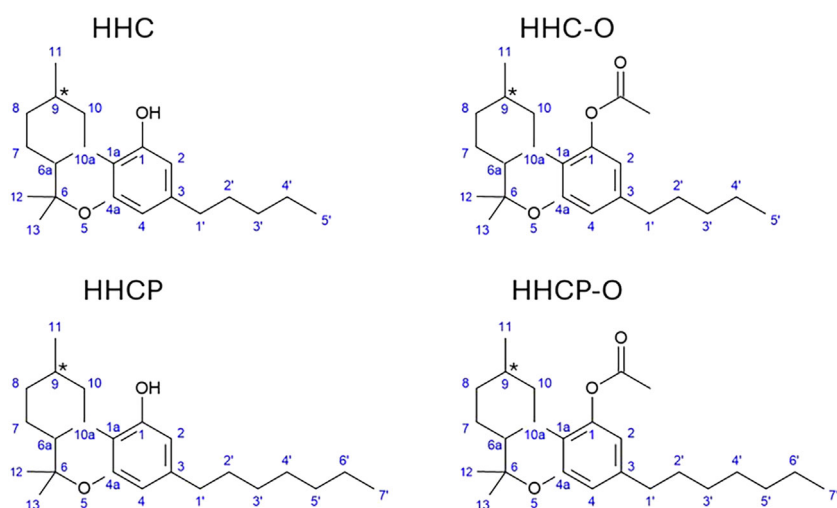


**FIGURE 1** Chemical structures with carbon numbers of semi-synthetic cannabinoids analysed in this study: HHC, HHC-O, HHCP and HHCP-O. \* indicates the position of the chiral centre for the main (9*R*) and (9*S*) epimers.

## 2 | METHODS

### 2.1 | Materials

The semi-synthetic cannabinoids (9R)- and (9S)-HHC, (9R)-HHCP, (9R)-HHC-O, (9R)-HHCP-O, 11-hydroxy-(9R)- and 11-hydroxy-(9S)-HHC, (8R)- and (8S)-hydroxy-(9R)-HHC, (8R)- and (8S)-hydroxy-(9S)-HHC and 11-carboxy-(9R)- and 11-carboxy-(9S)-HHC (purity  $\geq 98\%$ ) were purchased from Cayman Chemicals (Ann Arbor, MI, USA). The 5'-OH-HHC reference standard was synthesised in-house, and details of the synthesis and characterisation data can be found in the [Supporting Information](#). Acetonitrile (LC-MS grade), formic acid, methanol (LC-MS grade) and the reagents for the hepatocyte incubations, Williams E medium, L-glutamine and HEPES buffer were obtained from Thermo Fisher Scientific (Gothenburg, Sweden). Ethanol was from Kemetyl AB (Jordbro, Sweden). Cryopreserved primary human hepatocytes using the 20-donor pool and thawing medium (InVitroGro HT) were purchased from Bioreclamation IVT (Brussels, Belgium).

The internal standard solution for the urine samples (0.4  $\mu\text{g}/\text{mL}$  each of 11-nor-9-carboxy- $\Delta^9$ -THC-D9,  $\Delta^9$ -THC-D3, 11-hydroxy- $\Delta^9$ -THC-D3, cannabidiol-D3 and  $\Delta^9$ -tetrahydrocannabinolic acid A-D3) was prepared from reference material obtained from Cerilliant (Round Rock, TX, USA). Urine sample preparation used high-purity water made on site using a MilliQ Gradient production unit (Millipore, Billerica, MA, USA). Finden B-One  $\beta$ -glucuronidase was purchased from Kura Biotech, Puerto Varas, Chile.

### 2.2 | Hepatocyte incubations

Hepatocyte incubations and metabolite identification studies were performed as previously described<sup>19,20</sup> with slight modifications. In short, the 9R epimers of the cannabinoids were diluted to a working concentration of 10  $\mu\text{M}$  in Williams E medium, supplemented with HEPES buffer and L-glutamine. Pooled human hepatocytes (HHeps) were thawed to 37°C and added to 48 mL of InVitroGro HT medium. This solution was centrifuged at  $100 \times g$  for 5 min at room temperature, following which the supernatant was removed, and the pellet re-suspended in 50 mL of supplemented Williams E medium. The re-suspended pellet was centrifuged at  $100 \times g$  for 5 min at room temperature, the supernatant removed and the final pellet was re-suspended in Williams E medium with a cell concentration of  $2 \times 10^6$  cells/mL.

The HHeps were then incubated in an IncuLine® IL-10 digital incubator (VWR, Stockholm, Sweden) with the drug solutions (at a final concentration of 5  $\mu\text{M}$ ) in duplicates for 1, 3 and 5 h at 37°C. One hundred microlitres of ice-cold acetonitrile was added to stop the reactions. The samples were centrifuged at  $1100 \times g$  for 15 min at 4°C, and the supernatants were transferred to the injection plate for LC-QToF-MS analysis. Degradation controls (drug without HHeps) and negative controls (HHeps without drug) were also incubated for 5 h.

### 2.3 | Authentic urine samples

Cases sent to the National Board of Forensic Medicine between January and May 2023 were included in agreement with ethical approval from the Swedish Ethical Review Authority (2018/186:31). Urine samples were selected from cases that screened positive for cannabis in blood using an enzyme-linked immunosorbent assay (ELISA) but confirmed negative for THC, 11-OH-THC and 11-carboxy-THC and positive for HHC in blood.<sup>21</sup>

Urine samples were prepared as both non-hydrolysed and hydrolysed. The non-hydrolysed urine samples were prepared by combining 50  $\mu\text{L}$  urine with 50  $\mu\text{L}$  MilliQ water, 25  $\mu\text{L}$  methanol and 25  $\mu\text{L}$  internal standard in methanol (corresponding to 200 ng/mL of each compound). The hydrolysed urine samples were prepared by mixing 50  $\mu\text{L}$  urine with 50  $\mu\text{L}$  Kura B-One  $\beta$ -glucuronidase (room temperature) and incubating at room temperature for 2 h. Then, 25  $\mu\text{L}$  methanol and 25  $\mu\text{L}$  internal standard in methanol were added. Negative non-hydrolysed and hydrolysed urine samples and a mixture of B-One  $\beta$ -glucuronidase, MilliQ water and methanol were analysed as negative controls.

### 2.4 | Instrumental analysis

The analytical workflow was based on an established standardised protocol<sup>19,20</sup> to ensure comparability between substances and runs. Further optimisation with regards to collision energy, gradient and retention times were established using reference standards of the substances prior to the analysis. Optimisation was performed with the goal of producing molecular fragments of appropriate sizes (approximately 80–350  $m/z$ ) and to ensure the parent compound eluted between 10 and 13 min. As the resulting metabolites are generally more polar in nature than the parent, they usually elute prior to the parent compound. Due to the racemic composition of the substances in the urine samples, the analysis was also performed using methanol as a mobile phase to achieve a greater separation of the hydroxy and carboxy epimers.

The HHeps incubated and urine samples were analysed with a LC-QToF-MS system comprised of a 1290 Infinity UHPLC system (Agilent Technologies) coupled to a 6550 iFunnel QToF MS (Agilent Technologies) with a Dual Agilent Jet Stream electrospray ionisation source. Separation was achieved by injecting 10  $\mu\text{L}$  of the sample onto an Acquity HSS T3 column (150 mm  $\times$  2.1 mm, 1.8  $\mu\text{m}$ ; Waters, Sölleruna, Sweden) fitted with an Acquity VanGuard precolumn (Waters).

Mobile phase (A) consisted of water and (B) of acetonitrile both with the addition of 0.1% formic acid. For separation, the flow rate was 0.5 mL/min and the following gradient used: 10% B (0–0.6 min); 10% to 50% B (0.6–2 min); 50% to 90% B (2–13 min); 90% to 95% B (13–15 min); 95% B (15–18 min); 95% to 10% B (18–18.1 min); 10% B (18.1–19 min). The column temperature was 60°C. MS data were acquired using positive ionisation and an auto MS/MS acquisition with the following settings: scan range 100–950  $m/z$  (MS) and

**TABLE 1** (9R)-HHC, (9R)-HHC-O, (9R)-HHCP and (9R)-HHCP-O metabolites with biotransformation; molecular formulas; mean retention times (RT); accurate (calculated) masses of the protonated molecules; mass errors from all samples; peak areas after 1, 3 and 5 h incubations for two replicate samples; and major fragment ions (also indicative of biotransformation).

Met #	Biotransformation	Formula	Mean RT (min)	Accurate mass [M + H] <sup>+</sup> (m/z)	Mass error (ppm)		#1 peak area ( $\times 10^3$ )			#2 peak area ( $\times 10^3$ )			Major fragment ions
					Min	Max	1 h	3 h	5 h	1 h	3 h	5 h	
(9R)-HHC	C <sub>21</sub> H <sub>32</sub> O <sub>2</sub>	11.90	317.2474	-2.31	4.04	3910	44	50	24	46	42	81.0699, 193.1223, 207.1380, 231.1380	
H1 <sub>A</sub>	MonoOH + GLUC	4.89	509.2747	-1.01	0.98	489	1054	825	452	868	728	193.1223, 207.1380, 259.1700, 333.2424	
H1 <sub>B</sub>	MonoOH + GLUC	5.39	509.2748	-1.09	1.98	490	962	563	365	723	473	193.1223, 207.1380, 259.1700, 333.2424	
H2	Carboxylic acid (9R)	7.33	347.2218	-1.03	1.11	307	515	412	183	400	331	121.1012, 193.1223, 207.1380, 245.1536	
H3 <sub>A</sub>	DiOH + GLUC	3.21	525.2692	-1.85	1.32	112	244	276	109	225	279	135.1168, 191.1067, 209.1172, 275.1617	
H4	Dehyd + diOH + GLUC	5.29	523.2534	-1.27	0.09	743	191	189	50	157	176	193.1223, 207.1380, 219.1380, 301.2142	
H3 <sub>B</sub>	DiOH + GLUC	3.83	525.2692	-1.33	0.56	96	174	148	91	152	137	135.1168, 209.1172, 223.1329	
H3 <sub>C</sub>	DiOH + GLUC	3.42	525.2694	-2.23	1.34	59	113	107	58	103	105	191.1067, 209.1172, 257.1536	
H1 <sub>C</sub>	MonoOH + GLUC	4.39	509.2739	-2.16	0.73	30	51	36	24	46	29	193.1223, 219.1380	
(9R)-HHC-O	C <sub>23</sub> H <sub>34</sub> O <sub>3</sub>	14.00	359.2573	-3.71	-0.94	n.d.	n.d.	n.d.	36	n.d.	n.d.	193.1223, 207.1380, 317.2475	
HO1 <sub>A</sub>	Acetate loss + monoOH + GLUC	4.90	509.2732	-4.88	-1.70	179	619	783	187	538	618	193.1223, 207.1380, 259.1700, 333.2424	
HO1 <sub>B</sub>	Acetate loss + monoOH + GLUC	5.40	509.2730	-4.52	-2.53	58	317	427	79	285	289	193.1223, 207.1380, 219.1380, 333.2424	
HO2	Acetate loss + carboxylic acid (9R)	7.33	347.2209	-3.5	-1.29	74	296	367	81	308	218	193.1223, 207.1380, 245.1536, 301.2162	
HO3 <sub>A</sub>	Acetate loss + diOH + GLUC	3.21	525.2678	-4.05	-2.31	44	128	184	59	114	178	191.1067, 209.1172, 275.1617, 331.2268	
HO4	Acetate loss (9R)-HHC	11.90	317.2474	-3.76	-2.56	55	84	63	117	117	96	193.1223, 207.1380, 233.1536	
HO5	Acetate loss + dehyd + diOH + GLUC	5.29	523.2521	-3.92	-1.99	n.d.	93	145	n.d.	92	102	193.1223, 207.1380, 245.1536, 329.2111	
HO3 <sub>B</sub>	Acetate loss + diOH + GLUC	3.83	525.2675	-5.86	-2.35	28	83	99	26	78	80	209.1172, 223.1329	
HO3 <sub>C</sub>	Acetate loss + diOH + GLUC	3.45	525.2677	-6.86	-2.09	24	64	77	n.d.	52	68	191.1067, 257.1536	
(9R)-HHCP	C <sub>23</sub> H <sub>36</sub> O <sub>2</sub>	13.58	345.2792	-4.14	8.17	5340	546	3235	138	4578	4856	81.0699, 123.0441, 221.1536, 235.1692	
P1 <sub>A</sub>	MonoOH + GLUC	6.43	537.3090	4.31	7.27	325	1209	2119	454	970	1572	221.1536, 235.1692, 287.2006	
P2 <sub>A</sub>	DiOH + GLUC	3.72	553.3039	3.63	7.05	173	635	897	185	452	896	163.0754, 219.1380, 237.1485, 341.2475	

TABLE 1 (Continued)

Met #	Biotransformation	Formula	Mean RT (min)	Accurate mass [M + H] <sup>+</sup> (m/z)	Mass error (ppm)		#1 peak area (×10 <sup>3</sup> )			#2 peak area (×10 <sup>3</sup> )			Major fragment ions
					Min	Max	1 h	3 h	5 h	1 h	3 h	5 h	
P3	Dehyd + diOH	C <sub>23</sub> H <sub>34</sub> O <sub>4</sub>	9.27	375.2545	2.39	6.29	46	129	288	33	152	267	163.0754, 221.1536, 235.1692, 329.2475
P1 <sub>B</sub>	MonoOH + GLUC	C <sub>29</sub> H <sub>44</sub> O <sub>9</sub>	7.07	537.3084	3.09	6.99	77	144	132	186	163	184	221.1536, 247.1693, 287.2006, 361.1274
P4	Dehyd + triOH + GLUC	C <sub>29</sub> H <sub>42</sub> O <sub>11</sub>	3.58	567.2823	-0.04	6.68	19	76	112	12	50	149	121.1012, 233.1172, 275.1278, 355.2268
P2 <sub>B</sub>	DiOH + GLUC	C <sub>29</sub> H <sub>44</sub> O <sub>10</sub>	4.86	553.3036	2.46	7.71	14	60	108	19	42	75	237.1485, 251.1617, 303.1955
	(9R)-HHCP-O	C <sub>25</sub> H <sub>38</sub> O <sub>3</sub>	15.48	387.2894	-3.07	2.14	9	14	10	38	29	46	221.1536, 345.2788
PO1	Acetate loss + monoOH + GLUC	C <sub>29</sub> H <sub>44</sub> O <sub>9</sub>	6.44	537.3070	0.30	3.24	61	447	600	58	404	567	221.1536, 287.2006, 361.2737
PO2	Acetate loss + diOH + GLUC	C <sub>29</sub> H <sub>44</sub> O <sub>10</sub>	3.76	553.3013	-3.40	2.74	18	189	332	27	197	334	177.0910, 219.1380, 237.1485
PO3	Acetate loss (9R)-HHCP	C <sub>23</sub> H <sub>36</sub> O <sub>2</sub>	13.56	345.2795	-0.42	5.01	38	84	88	88	92	155	221.1536, 345.2788

Note: Metabolites are ordered from most to least abundant across all incubations. Abbreviation: n.d., not detected.

50–950 *m/z* (MS/MS); precursor intensity threshold of 5000 counts; precursor number per cycle, 5; fragmentor voltage, 380 V; CE, 3 eV at 0 *m/z* ramped up by 8 eV per 100 *m/z*; gas temperature, 150°C; gas flow, 18 L/min; nebuliser gas pressure, 345 kPa; sheath gas temperature, 375°C; and sheath gas flow, 11 L/min.

Hydrolysed urine samples were also analysed using mobile phases (A) water and (B) methanol, both supplemented with 0.1% formic acid. A longer gradient was used with a total run time of 26 min and the following gradient: 10% B (0–0.6 min); 10% to 50% B (0.6–2 min); 50% to 90% B (2–20 min); 90% to 95% B (20–23 min); 95% B (23–25 min); 95% to 10% B (25–25.1 min); 10% B (25.1–26 min). All other instrumental parameters were the same as described above.

## 2.5 | Data and statistical analysis

The data and statistical analysis comply with the recommendations on experimental design and analysis in pharmacology.<sup>22</sup> Agilent MassHunter Qualitative Analysis software (version B.07.00) was used for data analysis. The criteria for metabolite identification has been described previously,<sup>23</sup> but in brief, the data were searched for all the molecular formulas corresponding to potential modification of the parent compound by known biotransformations and any combinations thereof (up to three modifications). Each potential metabolite identification required mass errors <5 ppm for protonated molecules (values >5 ppm accepted for saturated or very small peaks, where the mass accuracy could deviate), a consistent isotopic pattern, a product ion spectrum consistent with the proposed structure and related to the parent compound, a retention time plausible for the proposed structure and the absence of identical peaks with the same mass spectrum in negative and degradation controls.

For the HHeps incubations, the total peak area for each metabolite was calculated by summing the peak areas for both replicates at all incubation times, which were then summed to calculate the total peak area for each parent compound. The total peak area of the parent compounds was not included in these calculations. For the urine samples, the total peak area for each metabolite was calculated by summing the peak areas for all samples, which were then summed to calculate the total peak area for all urine samples where HHC and/or its metabolites were identified. The total peak area of the parent compounds were included in these calculations. The percentage total peak areas were calculated using these values for different metabolites or biotransformations.

## 3 | RESULTS AND DISCUSSION

### 3.1 | Hepatocyte incubations

Following incubation with HHeps, eight metabolites were identified for (9R)-HHC, eight for (9R)-HHC-O, six for (9R)-HHCP and three for (9R)-HHCP-O. The identified metabolites are listed in Table 1. The metabolites are numbered according to their total peak area, from

highest to lowest. Proposed structures of the metabolites are organised in suggested metabolic pathways in Figures 2 and 3. The mass spectra and proposed fragmentation patterns of the parent compounds and all metabolites can be found in the [Supporting Information](#).

It should be noted that for (9R)-HHC and (9R)-HHCP, there are some large differences in peak areas between replicates for the parent and some metabolites. Given that the addition of an internal standard did not improve the stability, this variation is likely due to experimental variability, such as the saturation effect in the LC-QToF-MS detector, or the high lipophilicity of the compound, which may have led to some of the compound sticking to pipette tips or plastic incubation plates.

For the acetate analogues HHC-O and HHCP-O, all metabolites had acetate loss, resulting in similar metabolites with the same relative abundance as their non-acetate analogues HHC and HHCP, respectively. Therefore, the metabolites of HHC-O and HHCP-O will be discussed with the HHC and HHCP metabolites. As expected, this indicates that HHC-O and HHCP-O were first rapidly metabolised to HHC (HO4) and HHCP (PO3), respectively. Therefore, the use of HHC-O and HHCP-O is unlikely to be differentiated from that of HHC and HHCP, respectively, in biological samples, particularly urine. This is also likely to be true for other recently emerged acetate

analogues of other phytocannabinoids and semi-synthetic cannabinoids, including THC acetates and CBD di-acetate.<sup>30,31</sup> This may be problematic in jurisdictions where the acetate analogues are not controlled. In the future, authentic urine and other biological samples from people who have used phytocannabinoids and semi-synthetic cannabinoids should be examined in comparison with that of their acetate analogues to determine if their use can be differentiated.

### 3.2 | (9R)-HHC

In QToF-MS analysis, (9R)-HHC ( $m/z$  317.2474) was fragmented into three major product ions:  $m/z$  81.0699, representing the cyclohexyl ring;  $m/z$  193.1223, representing the aromatic ring and pentyl side chain; and  $m/z$  231.1380, representing the three-ring core. The observed fragment ions were used as the basis for elucidating the structures of the metabolites.

Following incubation with HHeps, eight metabolites were identified for (9R)-HHC and (9R)-HHC-O. The metabolites eluted between 3.21 and 7.33 min with the parent drug eluting at 11.90 min for (9R)-HHC and 14.00 min for (9R)-HHC-O (see Table 1). The observed biotransformations included monohydroxylations (monoOH), dihydroxylations (diOH), dehydrogenation (dehyd) in combination with

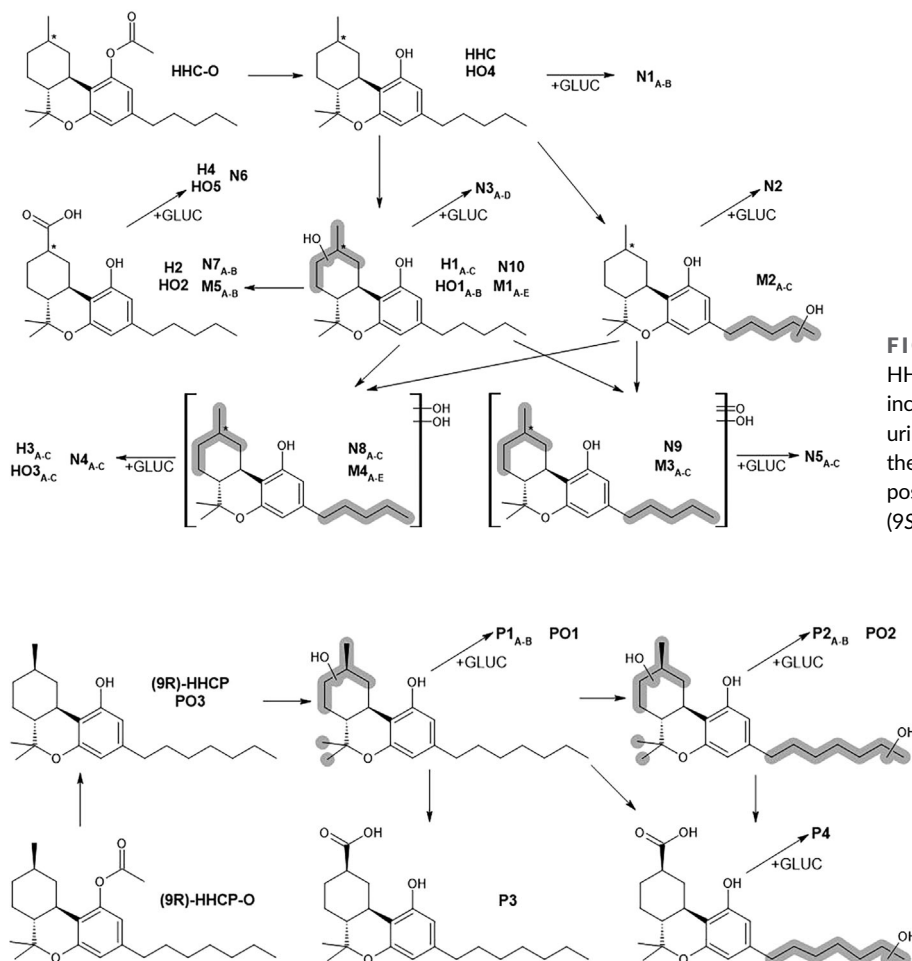


**FIGURE 2** Proposed metabolic pathways of HHC and HHC-O following duplicate 1, 3 and 5 h incubations with HHeps and analysis of authentic urine samples for HHC. Markush bonds represent the probable location of the group. \* indicates the position of the chiral centre for the main (9R) and (9S) epimers.

**FIGURE 3** Proposed metabolic pathways of (9R)-HHCP and (9R)-HHCP-O following duplicate 1, 3 and 5 h incubations with HHeps. Markush bonds represent the probable location of the group.

diOH (ketone or carboxylic acid formation) and glucuronidation (GLUC). All metabolites were glucuronidated except the metabolite formed from combined dehydrogenation and diOH (H2; HO2). The glucuronidations were characterised by the addition of  $m/z$  176 to the overall mass of the metabolites. All modifications occurred at either the cyclohexyl ring or pentyl side chain, where all identified metabolites had a biotransformation at the cyclohexyl ring and 37.5% of metabolites had a biotransformation at the pentyl side chain.

The two most abundant metabolites were produced via monoOH on the cyclohexyl ring and glucuronidation (H1<sub>A-B</sub>; HO1<sub>A-B</sub>). These metabolites were characterised by the addition of  $m/z$  16 to the parent, which is consistent with the addition of a hydroxy group. The absence of modifications to the fragment ions of the parent demonstrates the hydroxylations occurred on the cyclohexyl ring, although the exact locations of the hydroxy groups could not be determined as indicated by the Markush bonds in Figure 2.

Apart from glucuronidation, diOH was the most common biotransformation (H2-H4; HO2, HO3, HO5). The three metabolites with diOH combined with glucuronidation (H3<sub>A-C</sub>; HO3<sub>A-C</sub>) were found to have one hydroxy group added to the pentyl side chain and one added to the cyclohexyl ring. This was characterised by the addition of  $m/z$  32 to the overall mass, consistent with the addition of two hydroxyl groups, and the presence of a fragment ion at  $m/z$  209.1172, which indicates an addition of  $m/z$  16, consistent with one hydroxy group, to the aromatic ring and pentyl side chain mass fragment of the parent ( $m/z$  193.1223) with no further modifications. The remaining two metabolites with diOH were combined with dehydrogenation (H2 and H4; HO2 and HO5), representing the formation of a carboxylic acid on the cyclohexyl ring.

### 3.3 | (9R)-HHCP

(9R)-HHCP ( $m/z$  345.2792) was fragmented into three major product ions:  $m/z$  81.0699, representing the cyclohexyl ring;  $m/z$  123.0441, representing the aromatic ring; and  $m/z$  221.1536, representing the aromatic ring and heptyl side chain. The observed fragment ions were used as the basis for elucidating the structures of the metabolites.

Following incubation with HHepts, six metabolites were identified for (9R)-HHCP. The metabolites eluted between 3.58 and 9.27 min with the parent drug eluting at 13.58 min (see Table 1). The observed biotransformations included monoOH, diOH, dehydrogenation in combination with diOH (ketone or carboxylic acid formation), dehydrogenation in combination with trihydroxylation (triOH) and glucuronidation. Similar to HHC, all metabolites were glucuronidated, except the metabolite formed from combined dehydrogenation and diOH (P3). All modifications occurred at either the cyclohexyl ring or heptyl side chain, where all identified metabolites had a biotransformation at the cyclohexyl ring and half had a biotransformation at the heptyl side chain.

The most abundant metabolite was formed from monoOH and glucuronidation (P1<sub>A</sub>; PO1). The exact location of the monoOH on metabolites P1<sub>A-B</sub> and PO1 could not be determined but given no

modifications were observed on the major mass fragments of the parent, it was determined the hydroxy group was added to the cyclohexyl ring or isopropyl (carbons 12 or 13 on Figure 1).

Apart from glucuronidation, diOH was the most common biotransformation (P2<sub>A-B</sub> and P3; PO2). Two of the metabolites with diOH (P2<sub>A-B</sub>; PO2) had one hydroxy group added to the heptyl side chain and the other to the cyclohexyl ring or isopropyl. The other metabolite with diOH was combined with dehydrogenation (P3), representing the formation of a carboxylic acid on the cyclohexyl ring. The metabolite with triOH and dehydrogenation (P4) had a carboxylic acid on the cyclohexyl ring and a hydroxy group on the heptyl side chain.

Because HHC and HHCP produced similar metabolites, they likely follow a similar metabolic pathway. All modifications of HHC and HHCP occurred at either the cyclohexyl ring or pentyl side chain or isopropyl for HHCP; however, while all identified metabolites of both HHC and HHCP had a biotransformation at the cyclohexyl ring, HHCP showed greater biotransformation on the side chain, where half of its metabolites had a hydroxy group on the side chain in comparison to 37.5% of metabolites of HHC. This is likely due to the longer alkyl side chain of HHCP (heptyl) than HHC (pentyl). This relationship has been previously observed with phytocannabinoids, where tetrahydrocannabinolic acid (THCA) had greater metabolism on its pentyl side chain than the propyl side chain of tetrahydrocannabivarin (THCV).<sup>27</sup> This has also been identified in structure-metabolism relationships of synthetic cannabinoid receptor agonists (SCRAs), where greater metabolism on the alkyl chain tails has been observed for SCRAs with longer alkyl chains.<sup>28</sup>

### 3.4 | HHC authentic urine samples

The analysis of the non-hydrolysed and hydrolysed urine samples in acetonitrile resulted in the identification of 21 and 18 metabolites for HHC, respectively. The glucuronidated parent compound HHC (N1<sub>A-B</sub>) was identified in the non-hydrolysed samples (5.9% of total peak area) with both epimers being present, although it was not possible to determine which of the metabolites (N1<sub>A</sub> or N1<sub>B</sub>) corresponded to each epimer. The parent compounds (9R)- and (9S)-HHC were identified in the hydrolysed samples and confirmed with reference standards, where the (9S) epimer was found to be more abundant (1.8% of total peak area) than the (9R) epimer (1.3% of total peak area). The metabolites identified eluted between 3.20 and 7.63 min in non-hydrolysed urine samples and 4.00 and 9.51 min in the hydrolysed urine samples, with the parent drug HHC eluting at 11.69 (9S) and 11.79 min (9R). The identified metabolites are listed in Table 2 for the non-hydrolysed and Table 3 for the hydrolysed urine samples. Following the parent compounds, or glucuronidated parent compounds in the case of the non-hydrolysed urine samples, metabolites are numbered according to their prevalence in the urine samples, from the most to least prevalent, followed by abundance based on total peak areas across all samples. No HHC or metabolites were detected in Urine Sample 7 despite the corresponding blood sample containing



**TABLE 2** HHC metabolites identified in 16 non-hydrolysed urine samples with biotransformation, molecular formulas, mean retention times (RT), accurate (calculated) masses of the protonated molecules, mass errors from all samples, major fragment ions (also indicative of biotransformation) and peak areas for 16 urine samples.

Met #	Biotransformation	Formula	Mean RT (min)	Accurate mass [M + H] <sup>+</sup> (m/z)	Mass error (ppm)		Mass fragments
					Min	Max	
N1 <sub>A</sub>	HHC + GLUC	C <sub>27</sub> H <sub>40</sub> O <sub>8</sub>	6.68	493.2803	-2.17	3.92	193.1223, 317.2476
N1 <sub>B</sub>	HHC + GLUC	C <sub>27</sub> H <sub>40</sub> O <sub>8</sub>	6.92	493.2803	-1.72	3.44	193.1223, 317.2476
N2	MonoOH (side chain) + GLUC	C <sub>27</sub> H <sub>40</sub> O <sub>9</sub>	4.06	509.2750	-1.59	3.78	191.1067, 259.1693, 315.2319
N3 <sub>A</sub>	MonoOH (8) + GLUC	C <sub>27</sub> H <sub>40</sub> O <sub>9</sub>	3.90	509.2747	-4.26	3.76	193.1223, 259.1693, 315.2319
N3 <sub>B</sub>	MonoOH (11) + GLUC	C <sub>27</sub> H <sub>40</sub> O <sub>9</sub>	4.88	509.2753	-1.05	4.30	193.1223, 259.1693, 333.2424
N3 <sub>C</sub>	MonoOH (11) + GLUC	C <sub>27</sub> H <sub>40</sub> O <sub>9</sub>	5.35	509.2750	-3.19	3.89	193.1223, 259.1693, 333.2424
N4 <sub>A</sub>	DiOH + GLUC	C <sub>27</sub> H <sub>40</sub> O <sub>10</sub>	3.51	525.2703	-4.66	5.58	193.1223, 201.0910, 221.1536, 271.1692
N5 <sub>A</sub>	Dehyd + diOH + GLUC	C <sub>27</sub> H <sub>38</sub> O <sub>10</sub>	3.44	523.2535	-7.20	7.40	207.1016, 273.1485
N3 <sub>D</sub>	MonoOH (8) + GLUC	C <sub>27</sub> H <sub>40</sub> O <sub>9</sub>	3.98	509.2752	-5.26	5.66	193.1223, 233.1536, 259.1693, 315.2319
N6	Dehyd + diOH (carboxylic acid) + GLUC	C <sub>27</sub> H <sub>38</sub> O <sub>10</sub>	5.27	523.2541	-4.70	4.02	193.1223, 245.1536, 329.2111
N5 <sub>B</sub>	Dehyd + diOH + GLUC	C <sub>27</sub> H <sub>38</sub> O <sub>10</sub>	3.59	523.2533	-7.68	3.25	207.1016, 233.1177, 273.1485
N4 <sub>B</sub>	DiOH + GLUC	C <sub>27</sub> H <sub>40</sub> O <sub>10</sub>	3.42	525.2700	-6.08	4.76	191.1067, 257.1536
N4 <sub>C</sub>	DiOH + GLUC	C <sub>27</sub> H <sub>40</sub> O <sub>10</sub>	3.20	525.2700	-4.62	4.62	193.1223, 257.1536, 215.1067, 331.2268
N7 <sub>A</sub>	Carboxylic acid (9R)	C <sub>21</sub> H <sub>30</sub> O <sub>4</sub>	7.27	347.2220	-4.12	3.98	193.1223, 245.1536
N5 <sub>C</sub>	Dehyd + diOH + GLUC	C <sub>27</sub> H <sub>38</sub> O <sub>10</sub>	4.86	523.2533	-5.29	1.00	193.1223, 207.1016, 245.1536, 259.1693
N8 <sub>A</sub>	DiOH	C <sub>21</sub> H <sub>32</sub> O <sub>4</sub>	4.00	349.2380	0.61	3.41	191.1067, 215.1067, 257.1536
N9	Dehyd + diOH	C <sub>21</sub> H <sub>30</sub> O <sub>4</sub>	4.53	347.2222	-1.01	3.18	189.0910, 207.1016
N8 <sub>B</sub>	DiOH	C <sub>21</sub> H <sub>32</sub> O <sub>4</sub>	4.40	349.2384	2.37	3.82	191.1067, 275.1617
N8 <sub>C</sub>	DiOH	C <sub>21</sub> H <sub>32</sub> O <sub>4</sub>	4.13	349.2378	0.07	2.10	191.1067, 257.1536, 331.2268
N7 <sub>B</sub>	Carboxylic acid (9S)	C <sub>21</sub> H <sub>30</sub> O <sub>4</sub>	7.60	347.2223	0.82	3.82	193.1223, 259.1693, 301.2162
N10	MonoOH (11)	C <sub>21</sub> H <sub>32</sub> O <sub>3</sub>	7.63	333.2430	1.72	1.72	137.1325, 193.1223

Note: Following the glucuronidated parent compounds, metabolites are ordered from most to least prevalent, followed by abundance based on total peak area across all samples. Urine Sample 7 was not included in the table as no HHC or metabolites were found, despite being positive for HHC in blood.

TABLE 2 (Continued)

Met #	Peak area ( $\times 10^3$ ) in urine samples																
	1	2	3	4	5	6	8	9	10	11	12	13	14	15	16	17	
N1 <sub>A</sub>	n.d.	21	50	n.d.	138	20	n.d.	n.d.	n.d.	70	n.d.	n.d.	150	283	696	678	
N1 <sub>B</sub>	n.d.	n.d.	106	n.d.	93	n.d.	20	n.d.	n.d.	50	n.d.	n.d.	104	271	443	521	
N2	89	222	1073	50	226	256	393	182	137	475	176	80	581	295	2313	2034	
N3 <sub>A</sub>	164	115	405	22	52	213	113	126	108	323	88	44	312	131	852	1152	
N3 <sub>B</sub>	n.d.	51	806	64	301	206	224	114	195	477	141	29	451	694	1815	2370	
N3 <sub>C</sub>	n.d.	54	324	48	154	88	144	99	133	253	70	n.d.	96	494	1011	2183	
N4 <sub>A</sub>	98	110	n.d.	33	n.d.	258	260	88	120	314	102	35	127	174	1830	921	
N5 <sub>A</sub>	n.d.	40	2023	n.d.	44	120	199	58	130	311	124	81	187	93	273	841	
N3 <sub>D</sub>	71	90	351	32	106	n.d.	141	94	81	287	n.d.	n.d.	171	288	726	1037	
N6	n.d.	n.d.	473	n.d.	25	252	86	109	420	252	140	32	24	140	160	955	
N5 <sub>B</sub>	31	n.d.	321	26	n.d.	27	32	29	52	184	48	n.d.	99	39	160	252	
N4 <sub>B</sub>	58	89	1193	n.d.	58	n.d.	256	n.d.	160	519	297	63	244	330	n.d.	938	
N4 <sub>C</sub>	12	214	1831	n.d.	n.d.	n.d.	399	n.d.	250	872	n.d.	94	333	527	771	1445	
N7 <sub>A</sub>	n.d.	n.d.	255	n.d.	n.d.	74	n.d.	n.d.	100	n.d.	127	n.d.	n.d.	n.d.	419	140	
N5 <sub>C</sub>	n.d.	n.d.	340	27	n.d.	223	n.d.	66	n.d.	91	n.d.	n.d.	n.d.	n.d.	n.d.	n.d.	
N8 <sub>A</sub>	n.d.	n.d.	n.d.	n.d.	n.d.	n.d.	n.d.	n.d.	n.d.	n.d.	155	n.d.	n.d.	n.d.	1383	n.d.	
N9	n.d.	n.d.	60	n.d.	n.d.	n.d.	n.d.	n.d.	n.d.	n.d.	n.d.	n.d.	n.d.	n.d.	1309	n.d.	
N8 <sub>B</sub>	n.d.	n.d.	n.d.	n.d.	n.d.	n.d.	n.d.	n.d.	n.d.	n.d.	n.d.	n.d.	n.d.	n.d.	411	29	
N8 <sub>C</sub>	n.d.	n.d.	n.d.	n.d.	n.d.	n.d.	n.d.	n.d.	n.d.	n.d.	n.d.	n.d.	n.d.	n.d.	346	78	
N7 <sub>B</sub>	n.d.	n.d.	n.d.	n.d.	n.d.	n.d.	n.d.	n.d.	n.d.	n.d.	n.d.	n.d.	n.d.	n.d.	30	30	
N10	n.d.	n.d.	n.d.	n.d.	n.d.	n.d.	n.d.	n.d.	n.d.	n.d.	n.d.	n.d.	n.d.	n.d.	209	n.d.	

Note: Following the glucuronidated parent compounds, metabolites are ordered from most to least prevalent, followed by abundance based on total peak area across all samples. Urine Sample 7 was not included in the table as no HHC or metabolites were found, despite being positive for HHC in blood.

**TABLE 3** HHC metabolites identified in 16 hydrolysed urine samples with biotransformation, molecular formulas, mean retention times (RT), accurate masses of the protonated molecules, mass errors from all samples, major fragment ions (also indicative of biotransformation) and peak areas for 16 urine samples.

Met #	Biotransformation	Formula	Mean RT (min)	Accurate mass [M + H] <sup>+</sup> (m/z)	Mass error (ppm)		Mass fragments
					Min	Max	
	HHC (9S)	C <sub>21</sub> H <sub>32</sub> O <sub>2</sub>	11.69	317.2474	-1.35	1.43	98.0848, 193.1223
	HHC (9R)	C <sub>21</sub> H <sub>32</sub> O <sub>2</sub>	11.79	317.2474	-2.12	3.78	93.1223, 207.1380
M1 <sub>A</sub>	MonoOH (11)	C <sub>21</sub> H <sub>32</sub> O <sub>3</sub>	7.67	333.2425	-0.58	4.13	193.1223, 207.1380, 259.1693
M2 <sub>A</sub>	MonoOH (5'OH)	C <sub>21</sub> H <sub>32</sub> O <sub>3</sub>	7.09	333.2426	-0.75	4.95	191.1067, 209.1172, 259.1693
M2 <sub>B</sub>	MonoOH (side chain)	C <sub>21</sub> H <sub>32</sub> O <sub>3</sub>	7.37	333.2427	-3.37	2.69	191.1067, 259.1693, 315.2319
M3 <sub>A</sub>	Dehyd + diOH	C <sub>21</sub> H <sub>30</sub> O <sub>4</sub>	4.53	347.2222	-3.36	4.37	189.0910, 207.1016, 231.1016, 257.1536
M4 <sub>A</sub>	DiOH	C <sub>21</sub> H <sub>32</sub> O <sub>4</sub>	4.89	349.2374	-3.51	4.62	193.1223, 201.0910, 257.1536, 271.1692
M4 <sub>B</sub>	DiOH	C <sub>21</sub> H <sub>32</sub> O <sub>4</sub>	4.00	349.2379	-2.7	3.77	191.1067, 275.1617
M4 <sub>C</sub>	DiOH	C <sub>21</sub> H <sub>32</sub> O <sub>4</sub>	4.13	349.2379	-3.22	4.86	191.1067, 257.1536, 275.1617
M3 <sub>B</sub>	Dehyd + diOH	C <sub>21</sub> H <sub>30</sub> O <sub>4</sub>	4.78	347.2224	-2.92	5.62	177.0910, 207.1016, 273.1485
M3 <sub>C</sub>	Dehyd + diOH	C <sub>21</sub> H <sub>30</sub> O <sub>4</sub>	4.26	347.2222	-1.03	4.01	189.0910, 207.1016, 273.1485
M5 <sub>A</sub>	Carboxylic acid (R)	C <sub>21</sub> H <sub>30</sub> O <sub>4</sub>	7.27	347.2223	-0.91	5.95	193.1223, 207.1380, 245.1536, 301.2162
M5 <sub>B</sub>	Carboxylic acid (S)	C <sub>21</sub> H <sub>30</sub> O <sub>4</sub>	7.58	347.2219	-7.15	3.33	193.1223, 231.1380, 245.1536, 301.2162
M4 <sub>D</sub>	DiOH	C <sub>21</sub> H <sub>32</sub> O <sub>4</sub>	5.40	349.2375	-1.75	3.29	189.0910, 207.1016, 259.1693
M1 <sub>B</sub>	MonoOH (8)	C <sub>21</sub> H <sub>32</sub> O <sub>3</sub>	6.81	333.2424	-2.63	1.78	No spec
M2 <sub>C</sub>	MonoOH (side chain)	C <sub>21</sub> H <sub>32</sub> O <sub>3</sub>	5.80	333.2424	-1.82	3.55	191.1067, 209.1172, 259.1693
M4 <sub>E</sub>	DiOH	C <sub>21</sub> H <sub>32</sub> O <sub>4</sub>	4.40	349.2380	0.82	3.51	191.1067, 257.1536
M1 <sub>C</sub>	MonoOH	C <sub>21</sub> H <sub>32</sub> O <sub>3</sub>	9.51	333.2424	-1.63	1.72	193.1223, 221.1536, 259.1693, 315.2319
M1 <sub>D</sub>	MonoOH (8)	C <sub>21</sub> H <sub>32</sub> O <sub>3</sub>	7.04	333.2426	-0.75	0.61	193.1223, 233.1172, 259.1693, 315.2319
M1 <sub>E</sub>	MonoOH (8)	C <sub>21</sub> H <sub>32</sub> O <sub>3</sub>	6.65	333.2423	-0.61	0.42	193.1223, 233.1536, 259.1693, 315.2319

Note: Metabolites are ordered from most to least prevalent, followed by abundance based on total peak area across all samples. Urine Sample 7 was not included in the table as no HHC or metabolites were found, despite being positive for HHC in blood.

Abbreviation: n.d., not detected.

TABLE 3 (Continued)

Met #	Peak area ( $\times 10^3$ ) in urine samples																
	1	2	3	4	5	6	8	9	10	11	12	13	14	15	16	17	
	n.d.	n.d.	34	n.d.	95	n.d.	n.d.	n.d.	n.d.	45	n.d.	n.d.	96	187	470	419	
	n.d.	n.d.	72	n.d.	65	n.d.	n.d.	n.d.	n.d.	25	n.d.	n.d.	60	133	284	320	
M1 <sub>A</sub>	74	108	1182	119	503	251	347	220	304	651	208	55	544	1271	3662	5190	
M2 <sub>A</sub>	67	166	355	45	221	176	284	163	87	371	105	47	576	313	2168	1904	
M2 <sub>B</sub>	39	81	749	21	102	104	199	57	63	192	85	43	161	176	1248	701	
M3 <sub>A</sub>	65	74	3564	n.d.	28	120	528	49	159	381	380	102	324	225	1965	1762	
M4 <sub>A</sub>	75	134	527	127	52	88	406	198	116	623	178	n.d.	76	347	1428	974	
M4 <sub>B</sub>	56	n.d.	1217	n.d.	114	172	406	115	196	530	383	94	271	544	2739	1603	
M4 <sub>C</sub>	110	n.d.	1058	n.d.	128	129	298	52	112	255	205	75	130	243	729	699	
M3 <sub>B</sub>	47	42	705	n.d.	n.d.	22	177	82	110	318	140	49	214	229	757	775	
M3 <sub>C</sub>	n.d.	24	688	n.d.	n.d.	n.d.	279	n.d.	104	337	188	n.d.	100	153	1362	1156	
M5 <sub>A</sub>	n.d.	n.d.	271	n.d.	n.d.	70	51	25	239	28	177	n.d.	n.d.	121	461	711	
M5 <sub>B</sub>	n.d.	n.d.	58	82	n.d.	n.d.	22	n.d.	28	31	n.d.	n.d.	n.d.	41	74	222	
M4 <sub>B</sub>	n.d.	98	496	n.d.	n.d.	n.d.	338	n.d.	29	204	63	n.d.	n.d.	n.d.	868	229	
M1 <sub>B</sub>	22	n.d.	70	n.d.	n.d.	n.d.	24	n.d.	n.d.	51	n.d.	n.d.	49	n.d.	110	131	
M2 <sub>C</sub>	n.d.	n.d.	315	119	99	88	85	n.d.	n.d.	n.d.	23	n.d.	n.d.	n.d.	n.d.	n.d.	
M4 <sub>E</sub>	n.d.	n.d.	445	n.d.	n.d.	n.d.	n.d.	n.d.	n.d.	401	n.d.	n.d.	243	n.d.	1250	1326	
M1 <sub>C</sub>	n.d.	n.d.	n.d.	n.d.	n.d.	n.d.	n.d.	n.d.	n.d.	89	n.d.	n.d.	82	41	396	74	
M1 <sub>D</sub>	n.d.	n.d.	108	n.d.	n.d.	n.d.	n.d.	n.d.	n.d.	n.d.	n.d.	n.d.	n.d.	n.d.	374	430	
M1 <sub>E</sub>	n.d.	n.d.	n.d.	n.d.	n.d.	n.d.	n.d.	n.d.	n.d.	n.d.	n.d.	n.d.	n.d.	28	104	142	

Note: Metabolites are ordered from most to least prevalent, followed by abundance based on total peak area across all samples. Urine Sample 7 was not included in the table as no HHC or metabolites were found, despite being positive for HHC in blood.  
Abbreviation: n.d., not detected.

HHC, so this sample is not included in Table 2 or 3. The proposed metabolic pathways for HHC from analysis of non-hydrolysed and hydrolysed urine samples are shown in Figure 2.

Apart from glucuronidation, the same biotransformations were found in both the non-hydrolysed and hydrolysed urine samples, which consisted of monoOH, diOH and diOH in combination with dehydrogenation (ketone or carboxylic acid formation). The metabolites of HHC identified in authentic urine samples were also similar to the metabolites of HHC identified after incubation with HHeps, although there were more than double the number of metabolites in the urine samples. This is likely due to only the (9R)-HHC being incubated with HHeps in this study, whereas the urine samples contained metabolites of both epimers, as shown by the identification of both epimers of the parent compound (glucuronidated in non-hydrolysed) and multiple stereoisomers of metabolites, such as three stereoisomers of 8-OH-HHC, which were not identified in the samples from HHeps incubations. This is in agreement with previous studies that found HHC-containing products contain a mixture of both the (9R) and (9S) epimers.<sup>1,8,10-12</sup>

Similar to the metabolites from incubation with HHeps, 99.3% of hydroxylated metabolites were glucuronidated in the non-hydrolysed urine samples. Metabolites with monoOH in combination with glucuronidation were the most prevalent, accounting for 46.4% of the total peak area of the metabolites. A metabolite with a monoOH on the pentyl side chain (N2; 13.6% of total peak area) and a metabolite with a monoOH on the cyclohexyl ring, 8-OH-HHC (N3<sub>A</sub>; 6.7% of total peak area) were the only metabolites found in all 16 urine samples. Two 11-OH-HHC with glucuronide metabolites were the next most prevalent metabolites, found in 15 (N3<sub>B</sub>; 12.5% of total peak area) and 14 urine samples (N3<sub>C</sub>; 8.1% of total peak area). These are likely the (9R) and (9S) epimers of 11-OH-HHC, although it was not possible to determine which metabolite corresponded to which epimer. There were also two additional metabolites with a monoOH that were less prevalent and abundant, an 8-OH-HHC with glucuronide metabolite (N3<sub>D</sub>; 5.5% of total peak area) and a non-glucuronidated 11-OH-HHC metabolite (N10; 0.3% of total peak area).

The remaining 13 metabolites had a diOH, where 83.5% (based on total peak area) were glucuronidated. Three of these metabolites

had only diOH (N8<sub>A-C</sub>), three had diOH with a glucuronide (N4<sub>A-C</sub>), three had diOH in combination with dehydrogenation (N7<sub>A-B</sub>, N9) and four had diOH in combination with dehydrogenation and glucuronidation (N5<sub>A-C</sub>, N6). Two of the metabolites with diOH and dehydrogenation were confirmed by comparison with reference standards to be the (9R)- and (9S)-carboxylic acid metabolites (N7<sub>A</sub> and N7<sub>B</sub>, respectively). The remaining metabolites with diOH combined with dehydrogenation could not be confirmed but are presumed to be ketone formations.

Extensive glucuronidation was found in the non-hydrolysed urine samples and following HHeps incubation, which is similar to phytocannabinoids like THC.<sup>24-26</sup> In addition, Schirmer et al. (2023) found extensive glucuronidation of HHC metabolites in a urine sample collected 2 h after ingestion of HHC.<sup>15</sup> Unfortunately, glucuronidated parent compounds and metabolites are not available as certified reference standards. Because confirmation of identifications require comparison of the samples with certified reference standards, hydrolysing toxicological samples where use of these or other semi-synthetic cannabinoids is suspected is necessary.

The urine samples in this study were hydrolysed and an overlaid chromatogram from hydrolysed Urine Sample 17 is provided in Figure 4 to demonstrate the relative abundance and retention times of the identified metabolites and parent compound. No glucuronidated metabolites were identified in the hydrolysed urine samples, indicating complete hydrolysis. However, complete cleavage of glucuronides by  $\beta$ -glucuronidase was only achieved after using longer incubation times (2 h) than in the standard manufacturer recommended method of 15 min (data from standard incubation time not shown). The need for longer incubation times was also observed by Schirmer et al. (2023) where after hydrolysis of the urine sample, half of the metabolites (4 of 8) were still glucuronidated.<sup>15</sup>

The parent compound, (9R)- and (9S)-HHC, only accounted for 3.1% of the total peak area, demonstrating the extensive metabolism of HHC. Similar to the non-hydrolysed samples, metabolites with a monoOH were the most prevalent and abundant in the hydrolysed samples, accounting for 38.1% of the total peak area of identified metabolites. The 11-OH-HHC metabolite (M1<sub>A</sub>; 19.4% of total peak area) and two metabolites with a monoOH on the pentyl side chain

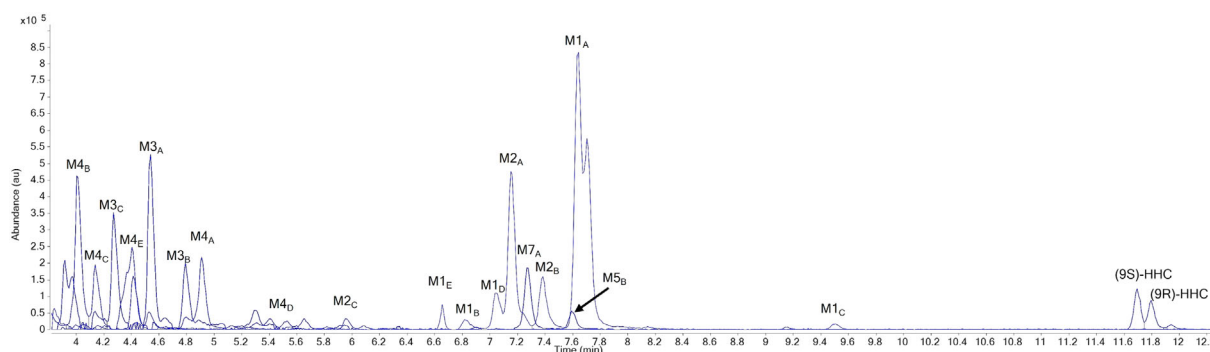


**FIGURE 4** The overlaid chromatogram of metabolites of HHC found in Urine Sample 17, demonstrating the abundance and retention times of all the metabolites.

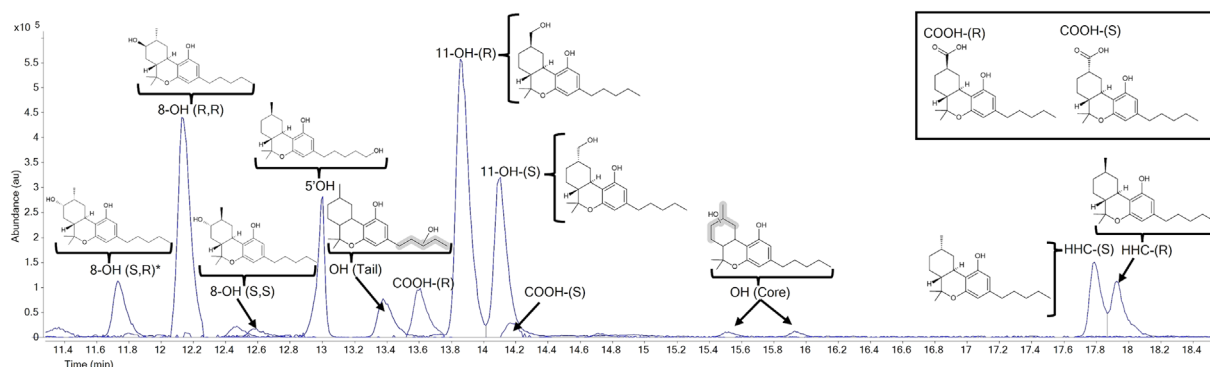


**FIGURE 5** The overlaid chromatogram and chemical structures of the epimers of HHC, 8-OH-HHC, 11-OH-HHC and carboxy-OH-HHC from running Urine Sample 17 in methanol with a longer gradient. \*This is presumed to be the (8*S*, 9*R*) epimer of 8-OH-HHC, although a reference standard was not available for confirmation.

(M2<sub>A</sub> and M2<sub>B</sub>; 9.3 and 5.3% of total peak area, respectively) were the only metabolites found in all 16 urine samples. There was a third metabolite with a monoOH on the pentyl side chain (M2<sub>C</sub>), but it was less abundant (1.0% of total peak area). In addition, although the 8-OH-HHC with glucuronide metabolite was the most prevalent and abundant in the non-hydrolysed urine samples, the three 8-OH-HHC metabolites identified in the hydrolysed urine samples (M1<sub>B</sub>, M1<sub>D</sub> and M1<sub>E</sub>) only accounted for 2.17% of the total peak area. There was also one additional monoOH metabolite (M1<sub>C</sub>) where the exact location of the hydroxy group could not be determined.

To confirm the locations and epimeric structure of the monoOH, two hydrolysed urine samples (16 and 17) were analysed alongside the reference standards using methanol and a longer gradient on the LC-QToF-MS to clarify the conformation. An overlaid chromatogram of Urine Sample 17 from the analysis with methanol is provided in Figure 5. As shown in Figure 5, both the (9*R*)- and (9*S*)-11-OH-HHC were confirmed to be present in the urine samples when run in methanol with a longer gradient, which improved separation of the epimers, whereas due to co-elution of the epimers, as can be seen in Figure 4, only one 11-OH-HHC metabolite (M1<sub>A</sub>) was identified when analysed using acetonitrile. Therefore, within the hydrolysed urine samples, the most prevalent and abundant metabolite for HHC was confirmed to be 11-OH-HHC (M1<sub>A</sub>). These results are consistent with prior studies of HHC metabolism. Manier et al. (2023) found a metabolite with monoOH in human plasma and following pooled human liver S9 fraction incubation of HHC, although the exact location of the monoOH was not confirmed.<sup>18</sup> In addition, Schirmer et al. (2023) identified both (9*R*)- and (9*S*)-11-OH-HHC as primary metabolites in urine<sup>15</sup> and Kobidze et al. (2024) identified (9*R*)-11-OH-HHC in urine.<sup>17</sup> It is also consistent with metabolism results of THC and CBD, where 11-OH-THC and 11-OH-CBD, respectively, are their principal metabolites. 11-OH-THC is an active metabolite,<sup>24,26,29</sup> so future work should examine if 11-OH-HHC also displays activity at the cannabinoid receptors.

Three stereoisomers of 8-OH-HHC, (8*R*, 9*S*), (8*S*, 9*S*) and (8*R*, 9*R*), were also confirmed to be present in varying amounts in the urine

samples. (8*S*)-OH-(9*R*)-HHC is also believed to present, although the reference standard was not available for confirmation. The (8*R*, 9*R*) and presumed (8*S*, 9*R*) epimers were found to be the most abundant of the 8-OH-HHC epimers. In comparison, Schirmer et al. (2023) only identified the (8*R*,9*R*)-8-OH-HHC epimer,<sup>15</sup> and Kobidze et al. (2023) identified no 8-OH-HHC metabolites but found 9 $\alpha$ -OH-HHC.<sup>17</sup> As can be seen in Figure 5, the epimers of the 8-OH-HHC metabolites predominantly correspond to (9*S*)-HHC, while the epimers of the 11-OH-HHC metabolites predominantly correspond to (9*R*)-HHC. It should be noted that similar to the 11-OH-HHC epimers, the 8-OH-HHC epimers could only be confirmed when run in methanol with a longer gradient. Further research might be conducted to improve the separation of the epimers, such as by using a chiral column and provide an opportunity for quantitative measurement of the epimers when all reference standards become available.

5'OH-HHC was also confirmed to be the most abundant metabolite with a monoOH on the pentyl side chain (M2<sub>A</sub>) following comparison with an in-house synthesised reference standard. Unfortunately, reference standards of the other isomers were not available for comparison, so the locations on the side chain of the hydroxylations for the other metabolites (M2<sub>B</sub> and M2<sub>C</sub>) could not be confirmed. In comparison, Schirmer et al. (2023) identified one metabolite with a monoOH on the pentyl side chain, which they tentatively identified to be at carbon four (4'OH-HHC).<sup>15</sup>

There were five metabolites with diOH (M4<sub>A-E</sub>) in the hydrolysed urine samples, which accounted for 31.7% of the total peak area, but the exact locations of the hydroxy groups were unable to be determined. There were also five metabolites with diOH in combination with dehydrogenation (M3<sub>A-C</sub> and M5<sub>A-B</sub>). Two of these metabolites were confirmed by comparison with reference standards to be the (9*R*)- and (9*S*)-carboxylic acid metabolites (M5<sub>A</sub> and M5<sub>B</sub>, respectively), where the (9*R*) epimer was found to be more abundant (2.9% of total peak area) than the (9*S*) epimer (0.7% of total peak area). The remaining metabolites with diOH combined with dehydrogenation (M3<sub>A-C</sub>; 23.52% of total peak area) could not be confirmed but are presumed to be ketone formations.

The (R)- and (S)-carboxylic acid metabolites of HHC (M5<sub>A</sub> and M5<sub>B</sub>, respectively) were only found in about half of the urine samples in this study (10 and eight urine samples, respectively) with relatively low abundance, whereas one other study found (9R)- and (9S)-11-COOH-HHC to be the most abundant metabolites in two urine samples.<sup>17</sup> Given the carboxylic acid metabolite of THC and CBD are their primary metabolites,<sup>24–26</sup> this indicates HHC may follow some of the same metabolic pathways as phytocannabinoids but that there are also some important differences. It should also be noted that none of the metabolites of HHC or HHCP were the same as those of THC or CBD, so the use of these semi-synthetic cannabinoids, which are currently not controlled in many jurisdictions, can be differentiated from the use of controlled phytocannabinoids.

## 4 | CONCLUSIONS

In this study, glucuronidation, hydroxylation and dehydrogenation were the only biotransformations identified for HHC and HHCP following incubation with HHeps and in authentic urine samples for HHC. HHC and HHCP were found to be extensively glucuronidated, where 99.3% of hydroxylated metabolites were glucuronidated in the non-hydrolysed urine samples. Metabolites with a monoOH were the most prevalent and abundant, accounting for 38.1% of the total peak area of identified metabolites in the hydrolysed urine samples. The 11-OH-HHC metabolite (M1<sub>A</sub>), 5'OH-HHC (M2<sub>A</sub>) and another metabolite with a monoOH on the pentyl side chain (M2<sub>B</sub>) were the only metabolites found in all 16 hydrolysed urine samples.

Given that 11-OH-HHC (M1<sub>A</sub>), 5'OH-HHC (M2<sub>A</sub>) and another metabolite with a monoOH on the pentyl side chain (M2<sub>B</sub>) were the only metabolites detected in all 16 urine samples where metabolites were identified, these metabolites along with the parent drug are suggested as suitable urinary markers to identify consumption of HHC and HHC-O. Following incubation with HHeps, the metabolites with monoOH + GLUC (P1<sub>A</sub>) and diOH + GLUC (P2<sub>A</sub>) were found to be the most abundant for HHCP and HHCP-O; therefore, these metabolites or their hydrolysed equivalents are suggested as suitable urinary markers to identify consumption of HHCP and HHCP-O. It is recommended that clinical and forensic toxicologists add these metabolites and characteristic ions to their targeted and semi-targeted analytical methods.

## AUTHOR CONTRIBUTIONS

**Conceptualisation:** Robert Kronstrand and Henrik Gréen. **Methodology:** Karin Lindbom, Steven Baginski, Lucas Krebs, Dartal Stalberga, Tobias Rautio, Xiongyu Wu, Robert Kronstrand and Henrik Gréen. **Data curation:** Karin Lindbom, Caitlyn Norman, Tobias Rautio and Robert Kronstrand. **Data analysis:** Karin Lindbom, Caitlyn Norman, Steven Baginski, Lucas Krebs, Dartal Stalberga, Tobias Rautio, Robert Kronstrand and Henrik Gréen. **Writing—original draft:** Karin Lindbom, Caitlyn Norman and Henrik Gréen. **Writing—review and editing:** All. **Supervision:** Robert Kronstrand and Henrik Gréen.

## ACKNOWLEDGEMENTS

The authors acknowledge Goodness Ogechi Akubiro for her assistance in the synthesis of 5'OH-HHC. This study received funding from the Eurostars-2 Joint Program (European Commission, E! 113377 [Eurostars-2], NPS-REFORM) with co-funding from the European Union's Horizon 2020 research and innovation programme, Sweden's Innovation Agency (Grant 2019-03566) and the Strategic Research Area in Forensic Sciences (Strategiombudet forensiska vetenskaper) at Linköping University. The Leverhulme Research Centre for Forensic Science is funded by the Leverhulme Trust (Grant RC-2015-011).

## CONFLICT OF INTEREST STATEMENT

The authors do not report any conflicts of interest.

## ORCID

Caitlyn Norman  <https://orcid.org/0000-0003-2322-0367>

Steven Baginski  <https://orcid.org/0000-0001-5615-1199>

Lucas Krebs  <https://orcid.org/0009-0005-7679-4403>

Darta Stalberga  <https://orcid.org/0000-0001-6712-652X>

Tobias Rautio  <https://orcid.org/0000-0002-0857-6261>

Xiongyu Wu  <https://orcid.org/0000-0001-6756-2276>

Robert Kronstrand  <https://orcid.org/0000-0002-4222-9597>

Henrik Gréen  <https://orcid.org/0000-0002-8015-5728>

## REFERENCES

- Ujváry I, Evans-Brown M, Gallegos A, et al. *Hexahydrocannabinol (HHC) and Related Substances*. Publications Office of the European Union; 2023.
- European Monitoring Centre for Drugs and Drug Addiction (EMCDDA). EU Early Warning System Formal Notification. [Notification of 6a,7,8,9,10,10a-hexahydro-6,6,9-trimethyl-3-pentyl-6H[1]dibenzo[b,d]pyran-1-ol (hexahydrocannabinol; HHC) in Europe.] EU-EWS-RCS-FN-2022-0031. 2022.
- European Monitoring Centre for Drugs and Drug Addiction (EMCDDA). EU Early Warning System Formal Notification. [Notification of (6,6,9-trimethyl-3-pentyl-6a,7,8,9,10,10a-hexahydrobenzo[c]chromen-1-yl) acetate (hexahydrocannabinol acetate; HHC acetate) in Europe.] EU-EWS-RCS-FN-2022-0035. 2022.
- European Monitoring Centre for Drugs and Drug Addiction (EMCDDA). EU Early Warning System Formal Notification. [Notification of 3-heptyl-6a,7,8,9,10,10a-hexahydro-6,6,9-trimethyl-6H-dibenzo[b,d]pyran-1-ol (hexahydrocannabinophorol; HHC-P) in Europe.] EU-EWS-RCS-FN-2023-0001. 2023.
- Erickson BE. Waiting for CBD regulations in the US. *Chem Eng News*. 2023;101(28):17–19. doi:10.1021/cen-10128-feature1
- Basas-Jaumandreu J, de las Heras FXC. GC-MS metabolite profile and identification of unusual homologous cannabinoids in high potency *Cannabis sativa*. *Planta Med*. 2020;86(5):338–347. doi:10.1055/a-1110-1045
- Citti C, Linciano P, Russo F, et al. A novel phytocannabinoid isolated from *Cannabis sativa* L. with an in vivo cannabimimetic activity higher than  $\Delta^9$ -tetrahydrocannabinol:  $\Delta^9$ -tetrahydrocannabinophorol. *Sci Rep*. 2019;9(1):20335. doi:10.1038/s41598-019-56785-1
- Russo F, Vandelli MA, Biagini G, et al. Synthesis and pharmacological activity of the epimers of hexahydrocannabinol (HHC). *Sci Rep*. 2023; 13(1):11061. doi:10.1038/s41598-023-38188-5
- Ujváry I. Hexahydrocannabinol and closely related semi-synthetic cannabinoids: a comprehensive review. *Drug Test Anal*. 2024;16(2): 127–161. doi:10.1002/dta.3519

10. Tanaka R, Kikura-Hanajiri R. Identification of hexahydrocannabinol (HHC), dihydro-iso-tetrahydrocannabinol (dihydro-iso-THC) and hexahydrocannabiphorol (HHCP) in electronic cigarette cartridge products. *Forensic Toxicol.* 2024;42(1):71-81. doi:10.1007/s11419-023-00667-9
11. Casati S, Rota P, Bergamaschi RF, et al. Hexahydrocannabinol on the light cannabis market: the latest "new" entry. *Cannabis Cannabinoid Res.* 2022;9(2):622-628. doi:10.1089/can.2022.0253
12. Höfert L, Becker S, Dreßler J, Baumann S. Quantification of (9R)- and (9S)-hexahydrocannabinol (HHC) via GC-MS in serum/plasma samples from drivers suspected of cannabis consumption and immunological detection of HHC and related substances in serum, urine, and saliva. *Drug Test Anal.* 2024;16(5):489-497. doi:10.1002/dta.3570
13. Ederly H, Grunfeld Y, Ben-Zvi Z, Mechoulam R. Structural requirements for cannabinoid activity. *Ann N Y Acad Sci.* 1971;191(1):40-53. doi:10.1111/j.1749-6632.1971.tb13985.x
14. Nasrallah DJ, Garg NK. Studies pertaining to the emerging cannabinoid hexahydrocannabinol (HHC). *ACS Chem Biol.* 2023;18(9):2023-2029. doi:10.1021/acscchembio.3c00254
15. Schirmer W, Auwärter V, Kaudewitz J, Schürch S, Weinmann W. Identification of human hexahydrocannabinol metabolites in urine. *Eur J Mass Spectrom.* 2023;29(5-6):1-12. doi:10.1177/14690667231200139
16. Harvey D, Brown N. Comparative in vitro metabolism of the cannabinoids. *Pharmacol Biochem Behav.* 1991;40(3):533-540. doi:10.1016/0091-3057(91)90359-A
17. Kobidze G, Sprega G, Montanari E, et al. The first LC-MS/MS stereoselective bioanalytical methods to quantitatively detect 9R- and 9S-hexahydrocannabinols and their metabolites in human blood, oral fluid and urine. *J Pharm Biomed Anal.* 2024;240:115918. doi:10.1016/j.jpba.2023.115918
18. Manier SK, Valdiviezo JA, Vollmer AC, Eckstein N, Meyer MR. Analytical toxicology of the semi-synthetic cannabinoid hexahydrocannabinol studied in human samples, pooled human liver S9 fraction, rat samples and drug products using HPLC-HRMS-MS. *J Anal Toxicol.* 2023;00(9):1-8. doi:10.1093/jat/bkad079
19. Watanabe S, Wu X, Dahlen J, et al. Metabolism of MMB022 and identification of dihydrodiol formation in vitro using synthesized standards. *Drug Test Anal.* 2020;12(10):1432-1441. doi:10.1002/dta.2888
20. Watanabe S, Vikingsson S, Åstrand A, Gréen H, Kronstrand R. Bio-transformation of the new synthetic cannabinoid with an alkene, MDMB-4en-PINACA, by human hepatocytes, human liver microsomes, and human urine and blood. *AAPS J.* 2020;22(1):13. doi:10.1208/s12248-019-0381-3
21. Kronstrand R, Roman M, Green H, Truver MT. Quantitation of hexahydrocannabinol (HHC) and metabolites in blood from DUID cases. *J Anal Toxicol.* 2024;48(4):235-241. doi:10.1093/jat/bkae030
22. Curtis MJ, Alexander S, Cirino G, et al. Experimental design and analysis and their reporting II: updated and simplified guidance for authors and peer reviewers. *Br J Pharmacol.* 2018;175(7):987-993. doi:10.1111/bph.14153
23. Kronstrand R, Norman C, Vikingsson S, et al. The metabolism of the synthetic cannabinoids ADB-BUTINACA and ADB-4en-PINACA and their detection in forensic toxicology casework and infused papers seized in prisons. *Drug Test Anal.* 2022;14(4):634-652. doi:10.1002/dta.3203
24. Chayasirisobhon S. Mechanisms of action and pharmacokinetics of cannabis. *Perm J.* 2021;25(1):1-4. doi:10.7812/TPP/19.200
25. Huestis MA. Human cannabinoid pharmacokinetics. *Chem Biodivers.* 2007;4(8):1770-1804. doi:10.1002/cbdv.200790152
26. Sharma P, Murthy P, Bharath MS. Chemistry, metabolism, and toxicology of cannabis: clinical implications. *Iran J Psychiatry.* 2012;7(4):149-156.
27. Rao Q, Zhang T, Pu Q-L, et al. Comparative metabolism of THCA and THCV using UHPLC-Q-Exactive Orbitrap-MS. *Xenobiotica.* 2023;53(1):46-59. doi:10.1080/00498254.2023.2194981
28. Baginski SR, Rautio T, Nisbet LA, et al. The metabolic profile of the synthetic cannabinoid receptor agonist ADB-HEXINACA using human hepatocytes, LC-QTOF-MS and synthesized reference standards. *J Anal Toxicol.* 2023;47(9):826-834. doi:10.1093/jat/bkad065
29. Lemberger L, Martz R, Rodda B, Forney R, Rowe H. Comparative pharmacology of  $\Delta^9$ -tetrahydrocannabinol and its metabolite, 11-OH- $\Delta^9$ -tetrahydrocannabinol. *J Clin Invest.* 1973;52(10):2411-2417. doi:10.1172/JCI107431
30. Holt AK, Poklis JL, Peace MR.  $\Delta^8$ -THC, THC-O acetates and CBD-di-O acetate: emerging synthetic cannabinoids found in commercially sold plant material and gummy edibles. *J Anal Toxicol.* 2022;46(8):940-948. doi:10.1093/jat/bkac036
31. Kruger DJ, Karahmet A, Kaplan SM, et al. A content analysis of social media discussions on THC-O-acetate. *Cannabis.* 2023;6:13-21. doi:10.26828/cannabis/2023/000164

## SUPPORTING INFORMATION

Additional supporting information can be found online in the Supporting Information section at the end of this article.

**How to cite this article:** Lindbom K, Norman C, Baginski S, et al. Human metabolism of the semi-synthetic cannabinoids hexahydrocannabinol, hexahydrocannabiphorol and their acetates using hepatocytes and urine samples. *Drug Test Anal.* 2024;1-15. doi:10.1002/dta.3740